JOURNAL OF MATERIALS SCIENCE 28 (1993) 4255–4260

Piezoelectric properties of niobium-doped 18PMN–41PZ–41PT ceramics

JIN-CHEN SHAW, KUO-SHUNG LIU, I-NAN LIN*
*Department of Materials Science and Engineering, and * Materials Science Centre, National Tsing Hua University, Hsin-Chu, Taiwan*

The effects of various amounts of excess niobium ions added to the 18PMN–41PZ–41PT three-component ceramics system on the crystal structure, microstructure, polarization versus electric field, strain versus electric field and piezoelectric properties, have been studied. It was found that addition of niobium ions to 18PMN–41PZ–41PT induced a change in the crystal structure from rhombohedral to tetragonal phase. The excessive niobium ions also formed a micro-second phase which existed in the grain boundary, which could refine and uniform the grain. The refined and uniformed microstructure was found to increase the remanent polarization, saturation strain, planar coupling coefficient, K_p, and mechanical quality factor, the best value of K_p being $\leqslant 69\%$.

1. Introduction

Lead zirconate–titanate ceramics, $Pb(Zr, Ti)O_3$, hold an excellent piezoelectric material position due to the many improvement studies carried out to date. Most of the improvements have been achieved either by partially replacing the constituent atom by other atoms, making up the pseudoternary solid solution compounds with other complex perovskite compounds, or doping with a small quantity of impurity additives [1–5].

The structure of PZT is perovskite (ABO_3). The impurity added may be classified as one of the ion valences being lower than those of the constituent atoms, where O-site vacancies are thus introduced by valence compensation. The other ion valence is higher than those ion valences of the constituent atom, where A-site vacancies are therefore introduced [6–8].

Niobium ions have been added to the 18PMN–41PZ–41PT three-component system and, therefore, the occupied B site of the ABO_3 perovskite structure. The piezoelectric properties have been studied with respect to microstructure, crystal structure P–E and S–E curves with varying amounts of niobium ions.

2. Experimental procedure

2.1. Composition selection

Ceramic of composition 18PMN–41PZ–41PT was taken as the base composition. The plain material came from the rhombohedral ferroelectric phase and showed maximum piezoelectric activity in the PMN–PZ–PT solid solution. Niobium ions were chosen as the doping impurity in quantities of 0, 1, 2, 4 and 8 mol %.

2.2. Ceramic sample preparation

The ceramic samples of the PMN–PZ–PT composition were prepared by the mixed oxides methods. The starting materials consisted of a high-purity PbO, ZrO_2, TiO_2, MgO and Nb_2O_5 of proper composition. The fine oxides were weighed by the molar composition. They were then wet-ball milled in ethanol for 8 h. The mixed powder was then dried and calcined at 850 °C in covered alumina crucibles for 6 h. The calcined powders then were wet-ball milled in ethanol with the addition of 0.5 wt % PVA for 8 h, dried and pulverized. The fine powders were pelletized at 12 mm diameter and 1–2 mm thick under a pressure of 1000 kg cm^{-2}.

The pellets were then sintered at 1250 °C for 1 h in sealed alumina crucibles. A PbO-rich atmosphere was maintained by placing $PbZrO_3$ inside the crucible in order to compensate for the PbO weight loss. Fired-on silver paint was applied to the fine polished surfaces of the sintered pellets and fired at 580 °C for 1 h. All the sintered samples were then poled in silicone oil at 120 °C for 20 min under a d.c. field of 3 kV cm^{-1}. Poled samples were aged for 24 h prior to property measurement.

2.3. Measurement

2.3.1. Structure

All the sintered samples were analysed with an X-ray diffractometer (Rigaku DMAX-II) using CuK_α radiation in order to identify their phases at room temperature.

2.3.2. Field-induced polarization

The polarization versus electric-field hysteresis loop was studied at room temperature, and at various field levels at 60 Hz using a modified Sawyer–Tower circuit [9].

0022–2461

2.3.3. Field-induced strain

The strain versus electric-field curve was measured under a low-frequency cycle time of 6 min. The strain was measured by a Michelson interferometer. The wavelength of the laser was 632.8 nm [10, 11].

2.3.4. Piezoelectric properties

The electromechanical coupling coefficient, K_p, and mechanical quality factor, Q_m, were calculated from

$$K_p = [2.51(f_a - f_r)/f_r)]^{1/2} \quad (1)$$

$$Q_m = [4\pi(f_a - f_r)RC]^{-1} \quad (2)$$

The resonant, f_r, and antiresonant, f_a, frequencies of the fundamental modes of the disc-samples were measured using an HP4194 impedance analyser.

3. Results and discussion

3.1. Crystal structure

The crystal structure of the 18PMN–41PZ–41PT was rhombohedral phase and the X-ray diffraction pattern of the niobium-ion doped sample is shown in Fig. 1a. The (2 0 0) X-ray peak was only observed at < 1 mol% niobium ions and the structure belonged to the rhombohedral phase. The (0 0 2) X-ray peak was found when the addition of niobium ions exceeded 1 mol %, where the structure had transformed to the tetragonal phase. The phase transformation from rhombohedral to tetragonal phase occurred when the niobium ion content was increased and the phase boundary lay between an addition of 1 and 2 mol % niobium ions.

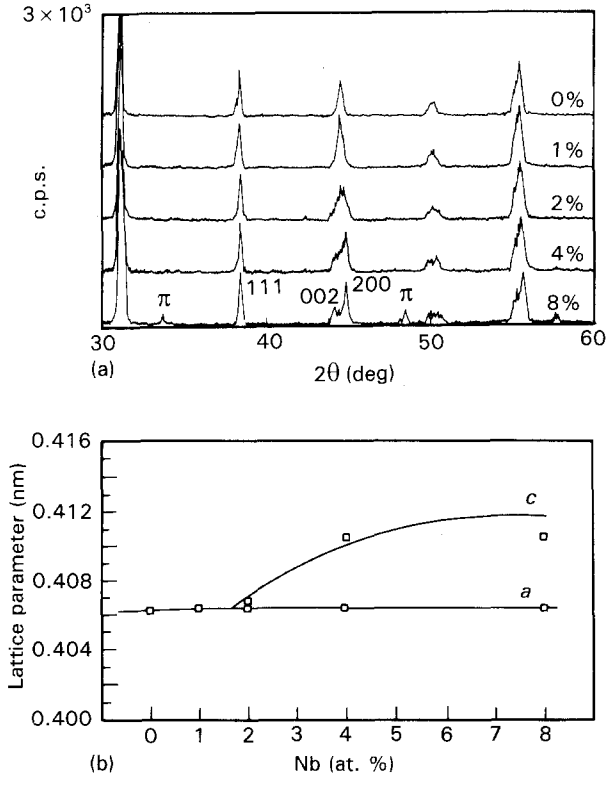

Figure 1 (a) The X-ray diffraction pattern for various niobium ion additions. (b) The variation of lattice parameter with Nb ion content.

When the niobium ion content was over 8 mol %, the second phase (pyrochlore phase) appeared and the amount (mol %) of pyrochlore phase could be calculated from [12]

$$\text{Pyro}(\%) = \frac{100I_{pyro}}{(I_{perov} + I_{pyro})} \quad (3)$$

where I_{pyro} and I_{perov} are the intensities of the major X-ray peaks (2 2 2) and (1 1 0) of the pyrochlore and perovskite phases, respectively. The pyrochlore phase content was 11 mol % when 8 mol % niobium ions was added to the 18PMN–41PZ–41PT sample. The 18–PMN–41PZ–41PT ferroelectric ceramics belongs to the pervskite structure (ABO_3). The addition of niobium ions directly affects the lattice parameter of the c-axis. Niobium ions added to 18PMN–41PZ–41PT ceramics are accommodated in the B site and then replace zirconium or titanium ions and thus affect the lattice parameter of the c-axis. The replacement of zirconium or titanium ions with niobium ions would induce A site vacancies in order to balance the charge. The lattice parameter of the a-axis is also affected.

The relationship between the lattice parameter and amounts of additional niobium ions is shown in Fig. 1b. The lattice parameter of the a-axis is unchanged; the lattice parameter of the c-axis, however, increased with increasing addition of niobium ions. The effect on the c-axis was larger than that on the a-axis when niobium ions were added. This is the reason for the crystal structure transformation from rhombohedral to tetragonal phase during the addition of increasing quantities of niobium ions, which occurred because the niobium ions increase the lattice parameter of the c-axis.

3.2. Microstructure

The microstructure of niobium-ion doped 18PMN–41PZ–41PT three-component system is shown in Fig. 2. The grain size of the 18PMN–41PZ–41PT sample was approximately 8–10 μm. The addition of 1 mol % niobium ions reduces the grain size to 1–2 μm. Further addition of niobium ions to 18PMN–41PZ–41PT reduces the grain size, but not significantly. Some pyrochlore phases found in the grain boundary occurred when 8 mol % niobium ions were added. The shape of pyrochlore was octahedral, and the grain size was larger than that on addition of 4 mol % niobium ions.

Some second phases in the PMN system are easily found when the ratio of Mg/Nb is smaller than 0.5: the Mg/Nb ratio is equal to 0.5 for 18PMN–41PZ–41PT, but it decreases when an amount of niobium ions is added to 18PMN–41PZ–41PT and the opportunity exists for it to form a micro-second phase in the grain boundary. This micro-second phase would prevent the grain boundary from moving during the sintering process. The second phase nucleates and grows when the quantity of second phase increases. The addition of 1 mol % niobium ions to 18MPN–41PZ–41PT could therefore clearly reduce the grain size. More niobium ions could

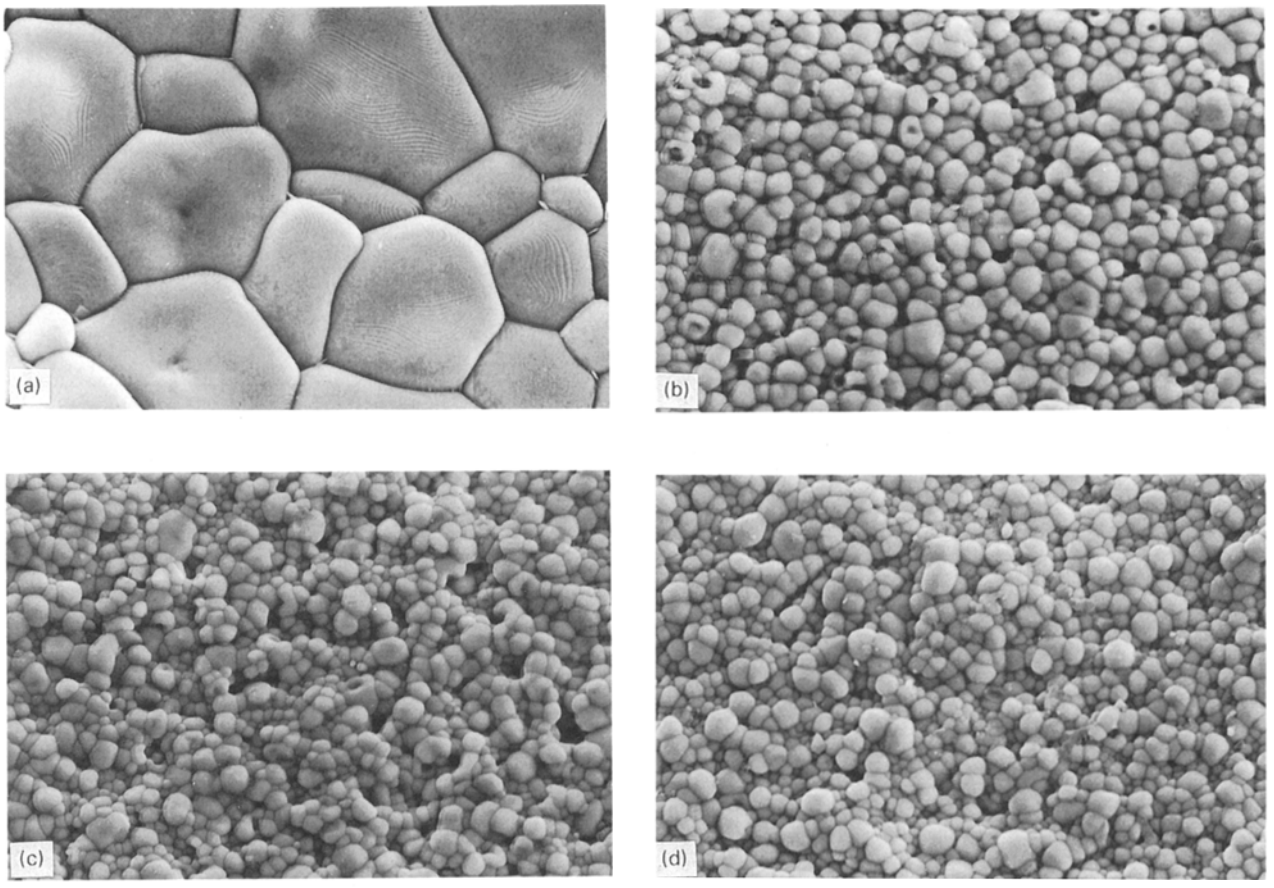

Figure 2 The variation of microstructure of 18PMN–41PZ–41PT with niobium ion content: (a) 0% (b) 1 mol %, (c) 2 mol %, (d) 4 mol %, (e) 8 mol %.

reduce grain size, but not significantly. The second phase nucleates and grows during the sintering process when the addition of niobium ions was more than 8 mol %. The grain again grows when the micro-second phase growth began, and the prevention of the grain boundary from moving would be lost.

3.3. Field-induced polarization

The structure of piezoelectric ceramics is perovskite (ABO_3) with a symmetrical centre (B site ion). The B-site ion can change its place when an alternating electric field is applied, inducing different polarizations at different places in the crystal. The polarization under an alternating electric field for the samples with different niobium-ion contents is shown in Fig. 3.

The poling direction of the tetragonal phase is $\langle 0\,0\,1 \rangle$ and has six different directions for reorientation at poling. The poling direction of the rhombohedral phase is $\langle 1\,1\,1 \rangle$ and has eight different directions for reorientation during poling [13, 14]. The rhombohedral phase has more reorientational direction than the tetragonal phase. The rhombohedral phase could then polarize more completely than the tetragonal phase, and could, therefore, achieve a larger remanent polarization. This result is shown in Fig. 4b.

The remanent polarization decreased when the grain size increased. Another reason for the decrease in remanent polarization was due to the second phase: 11 mol % second phase could reduce the remanent polarization by approximately 40%. Thus to achieve a large remanent polarization, the large grains and the existence of second phase should be avoided. The relationship between coercivity, E_c, and the niobium ion content is shown in Fig. 4a. The coercivity increased with increasing tetragonality. The effects of the grain size and second phase on coercivity were very small.

3.4. Field-induced strain

The B-site ion changed its place when the alternating electric field was applied, the movement of the B-site ion inducing lattice deformation. The relationship between the strain and the electric field (S–E curve) is shown in Fig. 5. The shape of the S–E curve can be separated into three parts: first, the rhombohedral

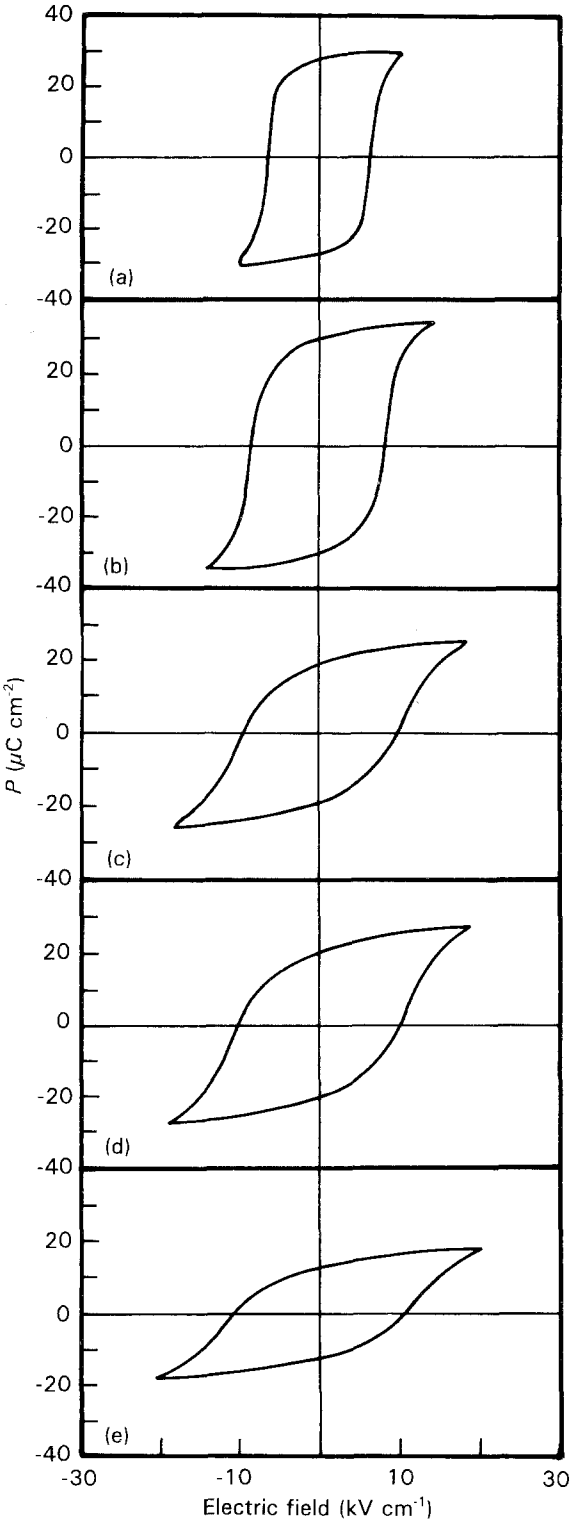

Figure 3 The polarization versus electric field for varying niobium ion contents: (a) 0%, (b) 1 mol %, (c) 2 mol %, (d) 4 mol %, (e) 8 mol %.

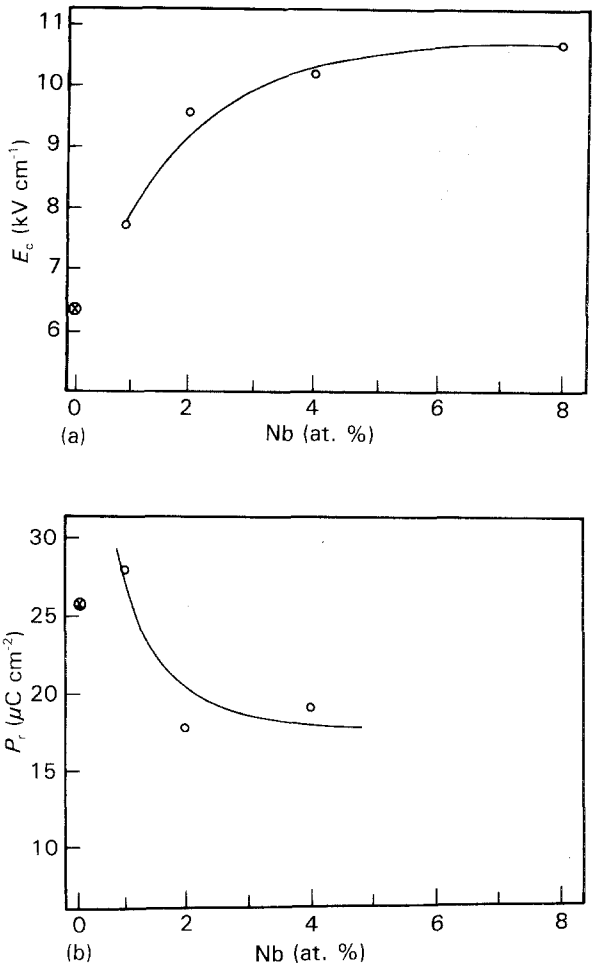

Figure 4 The relationship of niobium ion content with (a) E_c and (b) P_r for (⊗) 18 PMN–41PZ–41PT (undoped), and (○) niobium-doped samples.

phase, as shown in Fig. 5a and b; second, the tetragonal phase, shown in Fig. 5c and d; and third, the tetragonal containable second phase, shown in Fig. 5e.

The crystal structure of samples containing 0 and 1 mol % niobium ions belonged to the rhombohedral phase. However, a significant difference was seen in the shape of the *S–E* curve. The saturation strain on the addition of 1 mol % niobium ions was larger than that when no niobium ions were added, as shown in Fig. 6. Both samples had the same crystal structure, but their microstructures showed a significant difference. The addition of 1 mol % niobium ions produced a small (1–2 μm), uniform grain, compared with a large (8–10 μm), non-uniform grain in the undoped sample. Strain produced from the alternating electric field would be cancelled out by the non-uniform grain size and the large grain would make the reorientation of the dipole more difficult. The strain would therefore decrease when the grain size was increased.

Samples doped with 2 and 4 mol % niobium ions exhibited the same crystal structure and microstructure. The shape of the *S–E* curve was therefore very similar, as shown in Fig. 5c and d. The effect of the second phase on the *S–E* curve is shown in Fig. 5e. The effect of the second phase on the *S–E* curves is obviously observed.

The saturation strain of the rhombohedral phase was larger than that of the tetragonal phase of the same microstructure. The rhombohedral phase has eight reorientational directions whereas the tetragonal phase only has six reorientational directions. The dipole moment of the rhombohedral phase reoreientates more completely than that of the tetragonal phase under an alternating electrical field. The saturation strain of the rhombohedral phase was therefore significantly larger than that of the tetragonal phase.

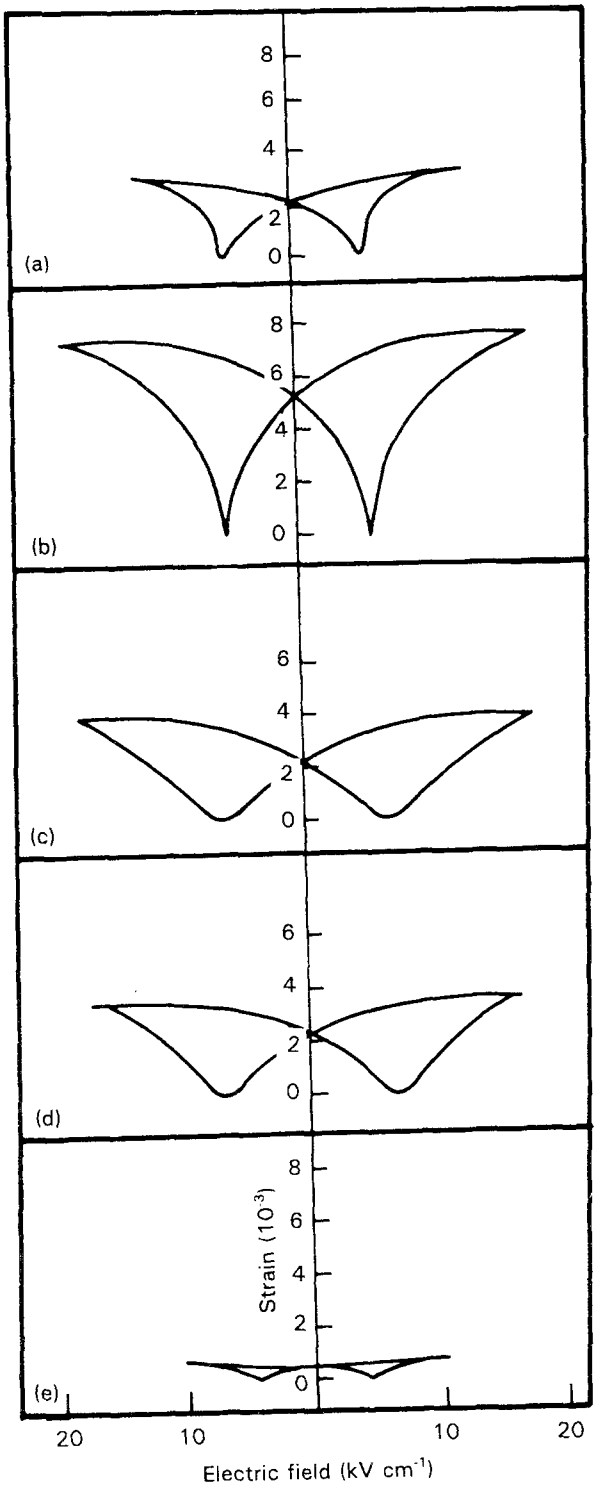

Figure 5 The variation of strain versus electric field with niobium ion content: (a) 0% (b) 1 mol %, (c) 2 mol %, (d) 4 mol %, (e) 8 mol %.

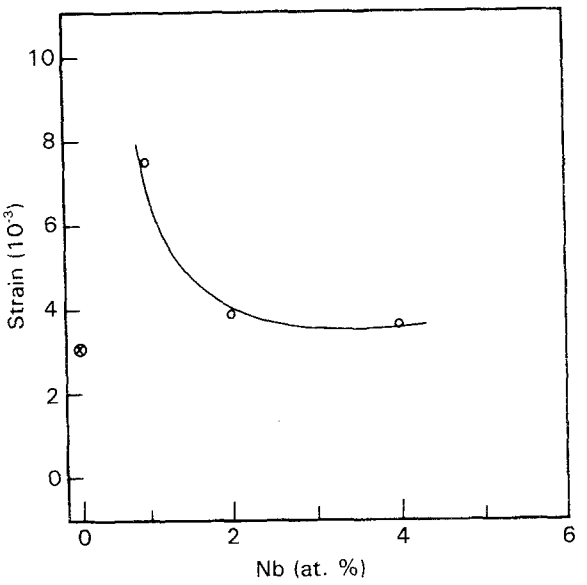

Figure 6 The relationship of saturation strain with niobium ion content: (⊗) undoped, and (○) doped 18 PMN–41PZ–41PT.

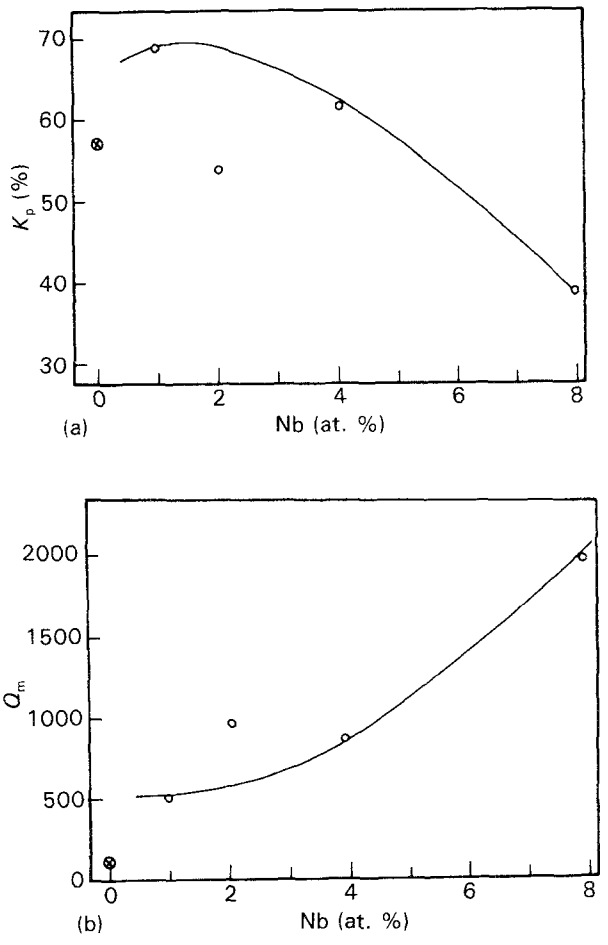

Figure 7 The relationship between niobium ion content: (a) K_p and (b) Q_m, in (⊗) undoped and (○) doped 18PMN–41PZ–41PT.

3.5. Piezoelectric properties

The relationship between planar coupling coefficient, K_p, mechanical quality factor, Q_m, and the amounts of niobium ions added is shown in Fig. 7a and b. The planar coupling coefficient increased with increasing niobium ion content. The reason why the addition of 1 mol % niobium ion produced the best K_p was that it had the most reorientational directions and uniform grain size, so that it could achieve the highest planar coupling coefficient. The best recorded value of K_p was $\leqslant 69\%$.

The mechanical quality factor, Q_m, increased with increasing niobium ion content. The mechanical loss, Q_m^{-1}, in ferroelectrical ceramics is primarily due to a dielectric loss. The dielectric loss, tanδ is considered to be the sum of macro-hysteresis loss, micro-hysteresis loss and intrinsic dielectric loss. The undoped sample had a large non-uniform grain size that would increase

the loss so that this sample had poor Q_m. The addition of niobium ions could produce a smaller, more uniform grain size, so that Q_m would increase with increasing addition of niobium ions.

4. Conclusions

1. The addition of niobium ions to 18PMN–41PZ–41PT ceramics increases the lattice parameter of the *c*-axis. The samples therefore allow a crystal structure transformation from rhombohedral to tetragonal phase with the addition of 1 and 2 mol % niobium ions.

2. The addition of a small amount of niobium ions produces a micro-second phase in the grain boundary, preventing the grain boundary from moving during the sintering process. Small amounts of niobium ions could, therefore, reduce the grain size. The second phase would nucleate and grow during the sintering process when more than 8 mol % niobium ions were added.

3. The rhombohedral phase has more reorientational directions than the tetragonal phase. It could therefore achieve a larger remanent polarization and strain than that of the tetragonal phase, caused by the larger grain and second phase, which would reduce the remanent polarization and strain.

4. A greater number of reorientational directions (rhombohedral phase) and a more uniform microstructure (on addition of 1 mol % niobium ions) produced a planar coupling coefficient, K_p, up to 69%. The mechanical quality factor, Q_m, increased with decreasing loss. Thus increasing the niobium ion content would then increase the value of Q_m.

Acknowledgement

We acknowledge the financial support for this research by the National Science Council, Taiwan, under Grant NSC81-0404-E0007-103.

References

1. MASAO TAKAHASHI, *Jpn J. Appl. Phys.* **9** (1970) 1236.
2. SADAYUKI TAKAHASHI and MASAO TAKAHASKI, *ibid.* **11** (1972) 31.
3. W. WERSING, *Ferroelectrics* **12** (1976) 143.
4. SADAYUKI TAKAHASHI, *Jpn J. Appl. Phys.* **20** (1981) 95.
5. R. HERBIET, U. ROBELS, H. DEDERICHS and G. ARLT, *Ferroelectrics* **98** (1989) 107.
6. L. EYRAUD, P. EYRAUD, P. GONNARD and M. TROCCAZ, *ibid.* **34** (1981) 133.
7. SADAYUKI TAKAHASHI, *ibid.* **41** (1971) 143.
8. RAMJILAL, S. C. SHARME and RAJIV DAYAL, *ibid.* **100** (1989) 43.
9. I. K. SINHA, *J. Sci. Instrum.* **42** (1965) 696.
10. W. Y. PAN, Q. M. ZHANG and Q. Y. JIANG and L. E. CROSS, *Ferroelectrics* **88** (1988).
11. Q. M. ZHANG, W. Y. PAN and L. E. CROSS, *J. Appl. Phys.* **63** (1988) 2492.
12. JOHN R. BELSICK, ARVIND HALLIYAL, UMESH KUMAR and ROBERT E. NEWNHAM, *Am. Ceram. Soc. Bull.* **66** (1987) 664.
13. M. J. HAUN, E. FURMAN, S. J. JANG and L. E. CROSS, *Ferroelectrics* **99** (1989) 13.
14. YA. KVAPULIN'SKI, Z. SUROV'YAK, M. F. KUPRIYANOV, S. M. ZAITSEV, A. YA. DANTSIGER and E. G. FESENKO, *Sov. Phys. Tech. Phys.* **24** (1979) 621.

Received 14 September 1992
and accepted 4 January 1993